LAWRENCE
LIVERMORE
NATIONAL
LABORATORY

LLNL-CONF-464133

Improving the Material Response for Slow Heat of Energetic Materials (U)

A. L. Nichols

December 16, 2010

NECDC 2010
Los Alamos, NM, United States
October 18, 2010 through October 22, 2010

Disclaimer

Improving the Material Response for Slow Heat of Energetic Materials (U)

Albert L. Nichols, III

Chemical Science Department
Lawrence Livermore National Laboratory, Livermore, CA 94550

Abstract. The goal of modern high explosive slow heat cookoff modeling is to understand the level of mechanical violence. This requires understanding the coupled thermal-mechanical-chemical system that such an environment creates. Recent advances have improved our ability to predict the time to event, and we have been making progress on predicting the mechanical response. By adding surface tension to the product gas pores in the high explosive, we have been able to reduce the current model's tendency to over-pressurize confinement vessels. We describe the model and demonstrate how it affects a LX-10 STEX experiment. Issues associated with current product gas equations of state are described and examined. (U)

Introduction

Understanding the response of energetic materials to adverse environments is an important component of predicting their hazard response. Over the past several years, we have been developing a fully coupled thermal-mechanical-chemical model for thermal explosion of HMX based materials[1,2,3]. In general, it is more difficult to predict the mechanical response of a slow heat experiment than a fast heat experiment. In the slow heat experiment large regions of the system are in an intermediate material state whose properties are more difficult to quantify experimentally. Because of this uncertainty, these models naturally undergo continual development. The kinetic reactions of the HMX are modeled with a reduced chemical reaction network developed by Nichols et al[4], which was calibrated to a number of small scale experiments. Each species in the reaction network has an equation of state and constitutive model that is combined to create an overall material model for the chemical mixture. The solid equations of state are based on fits to experimental data. The gas/fluid equations of state are derived from the CHEETAH equation of state code[5] with modification to take into account the liquid-gas co-existence region. In previous work, we added a porosity model to our chemical material model. The addition of the porosity model significantly improved the mechanical response of the chemical material in a thermally reacting environment by allowing the explosive to thermally expand into the pores without significantly increasing the pressure in confined systems. Although this model significantly improves the overall pressurization, it is still too high during the run up to the thermal explosion, and the pressure does not accelerate as rapidly as the experimental record.

In this paper we show the results of adding surface tension between the HE solid and the gases in the pores. The addition of the surface tension increases the confining force on the trapped gasses/he products, thereby reducing the overall pressure in the system. This allows more gas to be "stored" in the explosive matrix during the run up to explosion without over pressurizing the system. During the last stages of the run up to explosion, the increasing size of the pores reduces the confining force on the pore, leading to a rapidly increasing overall pressurization of the system.

We use our new model to model the slow heating STEX[6] experiment. We examine the difference between the mechanical/stress-strain response with and without the surface tension model and its implication for thermal/mechanical/chemical modeling of explosive systems.

Model Improvements

Surface Tension

Consider the effect of surface tension, σ_g, on a single gas pore in an explosive matrix. The volume, $V_{p,g}$, and area, $A_{p,g}$, of pore can be defined as $V_{p,g} = \gamma r^3$, $A_{p,g} = 3\gamma r^2$ for a suitable choice of topology factor γ and scale factor r. For a spherical pore, the topology factor is $\frac{4\pi}{3}$ and the scale factor is just the radius. If $E_{p,g}$ is the of the gas in the pore, then the total energy associated with a single pore is then

$$E_{p,g}^{tot} = E_{p,g} + 3\gamma\sigma_g r^2 \tag{1}$$

So in terms of the volume of gas in the pore, the total energy is:

$$E_{p,g}^{tot} = E_{p,g} + 3\gamma\sigma_g \left(\frac{\mathrm{V_{p,g}}}{\gamma}\right)^{\frac{2}{3}} = E_{p,g} + \tilde{\sigma}_g \left(\mathrm{V_{p,g}}\right)^{\frac{2}{3}} \tag{2}$$

Where $\tilde{\sigma}_g = 3\gamma^{\frac{1}{3}}\sigma_g$. The effective pressure seen by the surrounding media, $\widetilde{P_g}$, is simply the derivative of the energy with respect to volume:

$$\widetilde{P_g} = P_g - \frac{2}{3}\tilde{\sigma}_g \left(\frac{1}{\mathrm{V_{p,g}}}\right)^{1/3} \tag{3}$$

Now let us sum over all of the pores in the system. Let ω_g be the number of gas pores per reference volume, and V^0 be the reference volume. The total volume of gas is then

$$V_g = V^0 \omega_g V_{p,g} \tag{4}$$

Rearranging, we have

$$V_{p,g} = \frac{V_g}{V^0 \omega_g} = \frac{\alpha_g v}{\omega_g} \tag{5}$$

Here we have defined α_g as the volume fraction of g. We can define e_g and v_g as the energy and volume of gas per reference volume of gas, and v as the relative volume of the element, and surface tension factor $\bar{\sigma}_g = \tilde{\sigma}\omega_g^{\frac{1}{3}}$. Putting everything together, we have that the effective energy associated with all of the pores of gas, $\tilde{e}$ is:

$$\tilde{e}_g = e_g + v_g \bar{\sigma}_g \left(\frac{1}{\alpha_g v}\right)^{\frac{1}{3}} \tag{6}$$

And the effective pressure is

$$\tilde{P}_g = P_g - \frac{2\bar{\sigma}_g}{3(\alpha_g v)^{\frac{1}{3}}} \tag{7}$$

In order to solve for pressure temperature equilibrium, we need to know the thermodynamic derivatives of the gaseous species with surface tension. If x is either T_g or $\widetilde{P}_g$, then

$$\left(\frac{\partial x}{\partial \tilde{e}_g}\right)_{v_g} = \left(\frac{\partial x}{\partial e_g}\right)_{v_g} \left(\frac{\partial e_i}{\partial \tilde{e}_g}\right)_{v_g} = \left(\frac{\partial x}{\partial e_g}\right)_{v_g} \tag{8}$$

$$\left(\frac{\partial x}{\partial v_g}\right)_{\tilde{e}_g} = \left(\frac{\partial x}{\partial v_g}\right)_{e_g} - \left(\frac{\partial x}{\partial e_g}\right)_{v_g} \left(\frac{\partial \tilde{e}_g}{\partial v_g}\right)_{\mathrm{g}} \tag{9}$$

Thus the equation of state derivatives becomes:

$$\left(\frac{\partial T_g}{\partial \tilde{e}_g}\right)_{v_g} = \left(\frac{\partial T_g}{\partial e_g}\right)_{v_g} \tag{10}$$

$$\left(\frac{\partial \tilde{P}_g}{\partial \tilde{e}_g}\right)_{v_g} = \left(\frac{\partial P_g}{\partial e_g}\right)_{v_g} \tag{11}$$

$$\left(\frac{\partial \tilde{P}_g}{\partial v_g}\right)_{\tilde{e}_g} = \left(\frac{\partial P_g}{\partial v_g}\right)_{e_g} + \frac{2\bar{\sigma}_g}{9v_g(\alpha_g v)^{\frac{1}{3}}} - \frac{2\bar{\sigma}_g}{3(\alpha_g v)^{\frac{1}{3}}}\left(\frac{\partial P_g}{\partial e_g}\right)_{v_g} \quad (11)$$

$$\left(\frac{\partial T_g}{\partial v_g}\right)_{\tilde{e}_g} = \left(\frac{\partial T_g}{\partial v_g}\right)_{e_g} - \frac{2\bar{\sigma}_g}{3(\alpha_g v)^{\frac{1}{3}}}\left(\frac{\partial T_g}{\partial e_g}\right)_{v_g} \quad (12)$$

These models have been added to the ALE3D[7] chemical material model. The surface tension factor $\bar{\sigma}_g$ is applied to each species, so that the model can simulate a system with different types of pores. For example, one would expect that the pores associated with the initially trapped air will be larger than those that are created by the evolution of gas products.

Modifications to Implicit Mechanics to Handle the Chemical Porosity Model.

The porosity model in the chemical material model has been previously described with regard to examining hot spot formation for detonation.[8] One of the issues with that model, as described, is how it performs inside an implicit mechanics framework near the point where the pore yields. At such a point, the compressibility changes discontinuously, because on one side the material has an elastic response to compressing the pore, and on the other the pore is yielding plastically. Because of this discontinuity, and the fact that it has been difficult to derive the compressibility in the plastic region, we have replaced the analytic derivative with a central difference numerical derivative. This has several advantages. First, the derivative is an accurate representation of the adiabatic compressibility. Second, the volume variation used to define the derivative creates a natural smoothing from one branch to another. This latter effect is extremely important when the pore is yielding, since the end state of the equilibration is to have the pore just at the yield limit. Thus, the most prevalent state of a porous material under stress has one starting at the point with the discontinuity in the compressibility.

Time Step Control

One of the perennial problems associated with modeling a thermal run away is time step control. Typical time controls are related to the maximum temperature change, maximum mass fraction change, number of iterations required to solve the implicit problem, or simply the largest time step allowed. None of these time controls is entirely satisfactory. If the problem is being controlled by the number of iterations it took to solve the previous step, the time step will often oscillate because the number of iterations needed can be very non-linear in time. In general, one wants to optimize the time step so that one can compute the largest calculated time in the smallest amount of computer time. Thus one wants the time step to be small enough so that the problem is solved without too many non-linear iterations, but large enough so as not to take too many time steps.

The key to choosing a time step control for these non-linear problems is to determine which aspect of the problem leads to the most difficulty in the implicit solution. In our case, the composition is changing due to chemistry. However, not all composition change is as hard on the implicit solver. Thus, a composition change associated with a large volume change is more difficult to handle than one with a small volume change. Because of this difference, we added a new time constraint that is based on the volume fraction change predicted from the mass fraction change due to the chemical reaction and the current volume fraction. If one has a gas with a volume fraction to mass fraction ratio much larger than 1, as is typical during the initial gas production phase the simulation, this constrains the

time step more than the mass fraction change alone.

Effects of Surface Tension on the Gas Equation of State

One of the interesting effects of adding surface tension is the path in equation of state space that the gases take. Without surface tension, the tendency is for the gas to be initially formed at low temperature at a relatively large relative volume. As the temperature increases, more gas is formed into essentially a constant volume. This decreases the relative volume as the temperature increases. When one adds surface tension, the gas species are formed in the small pores that are being confined by the surface tension. The surface tension holds the gases in the pore and keeps the relative volume low. As more gas is formed, the pore is forced to increase in size, thereby reducing the retaining force on the pore. This causes the relative volume to initially increase. As more gas is formed, we again decrease the relative volume because of the increasing total quantity of gas.

One consequence of the change in the equation of state trajectory is that that path can send the material through a liquid-gas co-existence region. The phase change region is characterized by abrupt changes in derivative and potentially discontinuous material properties. In the context of an implicit mechanical solver, these properties can have a disastrous effect on the ability to find a stable solution.

Modeling the Scaled Thermal EXplosion (STEX) Experiment

These models have been inserted into the ALE3D code. To determine the effect of these models on the calculation of the response of a high explosive to a thermal environment, we examine the scaled thermal explosion experiment (STEX). The STEX system consists of a cylinder of high explosive inside steel confinement vessel made up of a relatively thin cylindrical wall connected to two stout

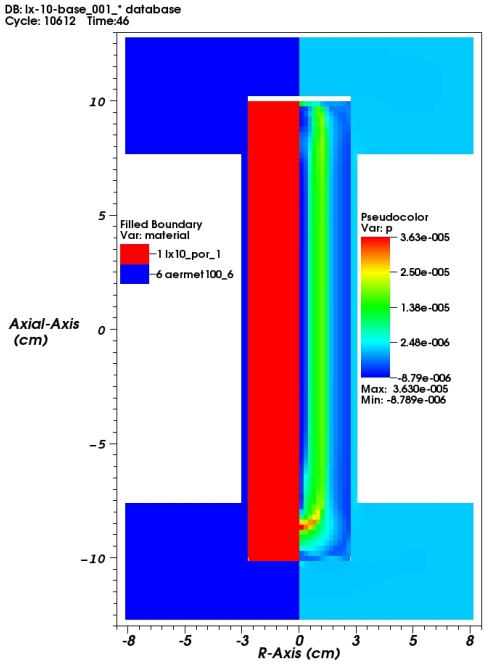

Fig 1. Configuration of the TE-47 STEX experiment and the pressure in the system at 46 hrs, between the point where the HE contacts the radial walls and make contact with the top.

end caps, as shown on the left side of Figure 1. We associate a temperature boundary condition on all outer external surfaces of the steel confinement vessel. This is a simplification of the experiment, where the temperature at the two end caps was several degrees less than that of the center. The explosive is simulated as a single cylinder, again a simplification from the experimental stack of essentially one inch tall, one inch radius parts. These simplifications help to reduce the computational complexity of the model for the purposes of this study, as the purpose of this study is to examine the effect of the material model changes.

In this paper, we are modeling the TE-47 STEX experiment. In that experiment, the explosive fill was LX-10. LX-10 consists of 95% HMX and 5% Viton-A. The solid material models are those developed by Yoh et.al.[1], and the reaction models are

those developed by Wemhoff et.al., based on work by Tarver and Tran, and Henson et.al.[9]. The model consists of 3 solid species, (β, δ, fragments), and 2 gaseous "species". The equation of state for the first "species" is based on the gaseous first fragments of the HMX decomposition, and the second is assumed to achieve full equilibration. These equations of state where developed in the CHEETAH code, and converted into tabular form to be used by the ALE3D code.

To set the value of the surface tension factor, $\bar{\sigma}$, we need both a surface tension for HMX and a pore number density. From Qasim et.al.[10], we have a value for the surface tension computed of 119 dyne/cm. In Behren's[11] work on the decomposition of HMX, he showed the existence of shells of decomposed HMX. The scale of those shells was clearly sub-micron, so we will use a length scale of a tenth of a micron for the base size scale for distance between pores. With these assumptions, we arrive at a value of $\bar{\sigma} = 5.8x10^{-5}\ Mb$. This will be our reference surface tension factor in all that follows. In the models considered here, we apply the surface tension factor to both HE product species but not the original air that is trapped in the solid matrix.

For the first set of calculations we analyze, we do not include results for models with the reference surface tension factor. This is because that model causes the code to attempt to evaluate the equation of state of the first gas product in the two phase co-existence region. As mentioned before, this causes the implicit solver to fail to solve, causing the problem to terminate at roughly the point where the HE starts making contact with the casing material.

To better understand what is going on with the TE-47 experiment, let us define the timeline. The external thermal profile started with a uniform 293 K, ramped to 403 K over 11 hours. It was then held at 403 K for 5 hours, and then ramped one degree per hour until the system exhibited thermal runaway. At roughly 45 hours, the HE cylinder made initial radial contact with the confinement wall, and made contact with the top surface about 4 hours later. It then sat and cooked until the system underwent thermal runaway and exploded after 68.4 hours. The right side of figure 1 we show the pressure in the STEX vessel after 46 hours. At this point, the $\beta \rightarrow \delta$ phase transition is roughly half way through the radius of the cylinder. Figure 1 shows that the pressure increases in the vicinity of the phase change as the material is trying to expand. That expansion places the neighboring material in tension, as witness the negative pressure in the core. This tension causes an axial restraint on the HE cylinder that effectively increases the radial expansion, increasing the hoop strain. Later, as the entire HE cylinder completes its transition to δ, that axial restraint is removed, allowing the cylinder to expand vertically and reducing the hoop strain.

First, we compare the thermal profile between the model without surface tension and the one with 10x the reference surface tension factor. For any time after the phase change temperature, the high surface tension model achieves the same temperature 10 minutes later than the model without surface tension. This shows that the introduction of the surface tension model does not have a significant adverse affect the time to explosion and the temperature profile of the STEX model.

Next we consider the effect of the surface tension model on the axial strain. In Figure 2, we show the axial strain during the last day of the TE-47 experiment. The experimental data is presented in the solid line, the dotted line is the simulation with no surface tension, and the dashed lines are 2, 5, and 10 times the reference surface tension factor defined above. Note that the model with no surface tension deviates from the experimental data roughly 24 hours before the thermal

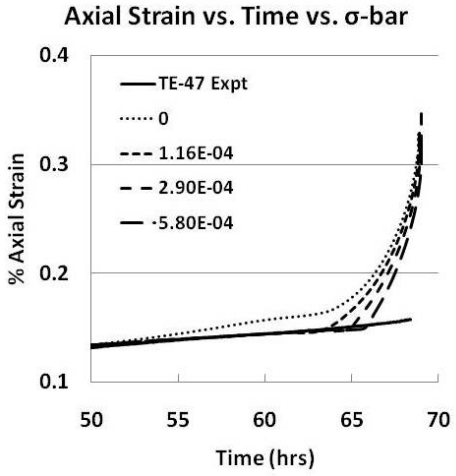

Fig 2. Axial strain vs. time. The solid line is the experimental data, the dotted line is with no surface tension model, and the other dashed lines are with increasing surface tension factor $\bar{\sigma}$. These values correspond to 0, 2, 5, and 10 times the reference surface tension factor defined in the text and are in Mb.

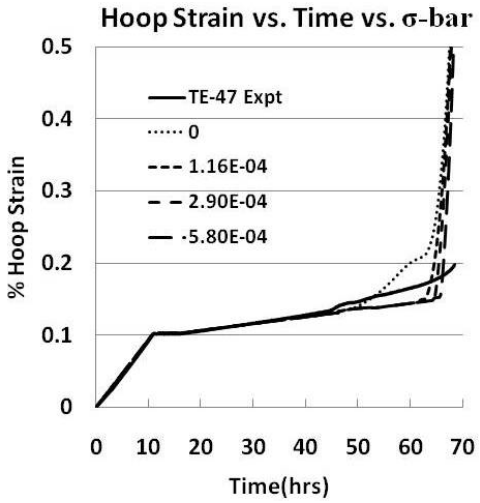

Fig 3. Hoop strain vs. time. The solid line is the experimental data, the dotted line is with no surface tension model, and the other dashed lines are with increasing surface tension factor $\bar{\sigma}$. These values correspond to 0, 2, 5, and 10 times the reference surface tension factor defined in the text and are in Mb.

runaway event, while for those with the surface tension model the deviation begins between two and four hours before the event, where the model with the highest surface tension factor having the smallest temporal error. This shows that the addition of the surface tension model significantly improves the axial strain response in the overall STEX model.

In Figure 3 we show the effect of the surface tension on the hoop strain for the TE-47 experiment, with the same models used and definitions used in the previous figure. Note that as we go from no surface tension to a factor of 2x, the strain response is notably reduced until the reaction runs away at the very end of the calculation. One interesting consequence of this new model is that where we were over shooting the strain after the 50 hour mark, we are now consistently undershooting it until the very end. The separation of the axial and hoop strain in the experiment probably indicates that there are strength effects that we have been able to neglect to this point, but will need to be addressed in further model developments.

In order to get a feel for how the surface tension effects the material response, we replaced the CHEETAH based initial HMX product gas with a JWL. The parameters used for the JWL are: $A = 107Mb$, $B = 2.34\ Mb$, $r_1 = 9.34$, $r_2 = 4.11$, and $\omega = 0.89$. The JWL form used is defined by:

$$P = Ae^{-r_1 v} + Be^{-r_2 v} + \frac{\omega C_v T}{v} \qquad (13)$$

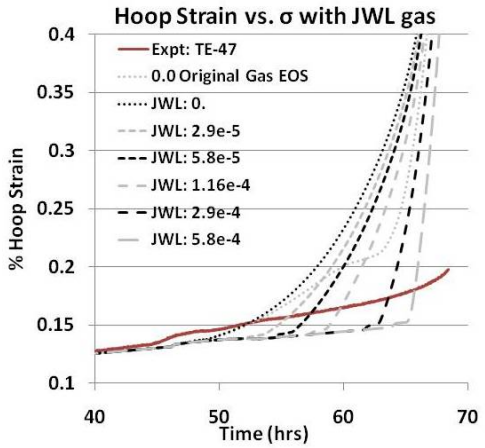

Fig 4. Comparison of the hoop strain replacing the original models CHEETAH eos with a JWL fit. This shows that the strain suppression in Fig 3 is due to the existence of a liquid-gas phase change.

Using this new product equation of state, we reran the 0, 0.5, 1, 2, 5, and 10 times the reference surface tension factor, and show the hoop strain in Fig 4. By comparing the difference in the hoop strain between the two zero surface tension models, we see that the initial product gas equation of state has had a significant impact on our ability to model this system. The strain curves with the increasing surface tension show that the surface tension model essentially reduces the pressure seen in the surrounding media. The reason that the previous models had such a drastic change is because the surface tension caused the gaseous species to phase change to the liquid phase.

Conclusions

In this paper we have shown the effect of adding surface tension between the HE product gasses and the HE solid. Depending on the strength of that effect, it can reduce the strain on the confining vessel without significant adverse effect on the reaction timing. By considering a simpler equation of state for the initial gaseous product, we found that a significant cause for the improved mechanical response is that the surface tension increases the pressure on the gaseous components enough to force them to condense to the liquid phase. This dependence on the liquid-gas phase change in the explosive products can lead to mechanical stability issues that will need to be addressed in the future if one desires to solve more general problems with an implicit mechanics model.

Currently, this surface tension model assumes that the gaseous components are in uniformly sized pores. In a real system, these pores could have a broad size distribution. In that case, a small amount of gas in large pores would cause the overall pressure in the system to be between the calculations with and without surface tension, making the system appear to have less gas present than the original model without surface tension. Such a physical effect could be the source of the current discrepancy.

Clearly, work needs to be done to improve the handling of materials that exhibit a phase change in the accessible phase space of the simulation. This includes understanding the strength properties of these PBX materials at high temperatures past the $\beta \rightarrow \delta$ phase change.

Overall, we have demonstrated significant improvements in the mechanical response of a high explosive system subjected to a slow thermal cook-off environment. The temperature error has not been degraded due to the new model, and the pressure/strain error has been significantly reduced, to where the error is limited to only the last few hours of the calculation. This model suggests that we are getting closer to the goal of being able to predict reaction violence for thermally driven events.

Acknowledgements

The author would like to thank Rich Behrens for useful discussions as this model was being developed. I would also

like to thank the ALE3D team for providing the framework and support for the development of this model. This work performed under the auspices of the U.S. Department of Energy by Lawrence Livermore National Laboratory under Contract DE-AC52-07NA27344.

References

1. Yoh, J. J., et. al., "Simulating Thermal Explosion of Octahydrotetranitrotetrazine (HMX)-based Explosives: Model Comparison with Experiment,: J. Appl. Phys. 100, 073515, 2006

2. Tarver, C. M., and Tran, T. D., "Thermal Decomposition Models for HMX-based Plastic Bonded Explosives," Combustion and Flame, 137, 50, 2004.

3 Wemhoff, A. P., Howard, W. M., Burnham, A. K., and Nichols III, A. L. (2008) An LX-10 Model Calibrated Using Simulations of Multiple Small-Scale Thermal Safety Tests, *Journal of Physical Chemistry A*, Vol. 112, pp. 9005-9011

4. Nichols, A. L. III, "Toward Improved Fidelity of Thermal Explosion Simulations", Shock Compression of Condensed Matter-2009, AIP Conference Proceedings, Nashville, TN, 2009, p 229.

5. Fried, L. L., et. al., "Cheetah 3.0 User's Manual", Lawrence Livermore National Laboratory Report, UCRL-MA-117541-Rev-6, 2000

6 Wardell, J. F., and Maienschein, J. L., "The Scaled Thermal Explosion Experiment," *Proceedings of 12th International Detonation Symposium*, San Diego, CA, Office of Naval Research, 2002

7 Nichols, A. L. III, Editor, "User's Manual for ALE3D, An Arbitrary Lagrange/Eularian 2D and 3D Code System", Lawrence Livermore National Laboratory LLNL-SM-404490 Rev 1, 2009.

8 Nichols, A. L. III, "A Model for Thermal Cook-off and Explosion of High Explosive", *Proceedings of the 13th International Detonation Symposium*, pp1151-1160, Norfolk, VA, Office of Naval Research, 2006.

9 Henson, B. F., et. al., J. Chem. Phys. 117, 3780, 2002

10 Qasim, M., Uchimiya, M., Gorb, L., Leszczynski, J., Moore, B., Taylor, L., Middleton, M., "Common Trends in the Relationships between Chemical and Physical Properties and Molecular Structure of Nitramine, Cage Nitramine, and Notroaromatic Energetics", *Proceedings of the 26th Army Science Conference*, Orlando, FL, Dec 2008.

11 Behrens, R., "Thermal Decomposition of HMX: Morphological and Chemical Changes Induced at Slow Decomposition Rates", *Proceedings of 12th International Detonation Symposium*, San Diego, CA, Office of Naval Research, 2002